Explicit Discontinuous Deformation Analysis Method with Lumped Mass Matrix for Highly Discrete Block System

Yongtao Yang[1]; Dongdong Xu[2]; and Hong Zheng[3]

Abstract: In the traditional discontinuous deformation analysis (DDA) method, the implicit time integration scheme is used to integrate equations of motion for modeling the mechanical behavior of a highly discrete rock block system. This requires that global equations be constantly solved. Hence, the computational efficiency of the traditional DDA method will decrease, especially when large-scale discontinuous problems are involved. Based on the explicit time integration scheme, an explicit version of the DDA (EDDA) method is proposed to improve computational efficiency of the traditional DDA method. Since a lumped mass matrix is used, there is no need to assemble global mass and stiffness matrices. More importantly, solving large-scale simultaneous algebraic equations can be avoided. The open–close iteration, which can assure the correct arrangement of constraints, is kept in the EDDA method. In addition, the simplex integration method, which is capable of conducting exact integration over an arbitrarily shaped block, is employed. Two numerical examples, including a sliding problem with an analytical solution and an underground cavern, are solved. The numerical results indicate the accuracy and robustness of the proposed EDDA method. **DOI: 10.1061/(ASCE)GM.1943-5622.0001234.**

Author keywords: Discontinuous deformation analysis (DDA) method; Explicit discontinuous deformation analysis (EDDA) method; Lumped mass matrix; Implicit time integration scheme; Explicit time integration scheme; Numerical manifold method (NMM).

Introduction

Due to long-time geologic effects, natural rock masses have been cut by various of structural planes (joints, faults, and weak-side) into discontinuous rock masses. Accurately studying the mechanical behavior of discontinuous rock block systems under different loading conditions using analytical, semianalytical, and experimental methods is very difficult. Therefore, many effective numerical methods such as the finite-element method (FEM) (Desai et al. 1984; Goodman and John 1977; Katona 1983; Zienkiewicz and Taylor 2000; Yang et al. 2017b), the boundary element method (BEM) (Beskos 1997), the discrete element method (DEM) (Cundall 1971), the FEM/DEM (Barla et al. 2012; Mahabadi et al. 2012; Elmo et al. 2013; Ma et al. 2014; Munjiza 2004; Antolini et al. 2016; Yan and Zheng 2017a, b), and the numerical manifold method (NMM) (Shi 1991; Ning et al. 2011; Wong and Wu 2014; Zhang et al. 2010; Fan et al. 2013; Zheng et al. 2013, 2014a; Zheng and Xu 2014; Zheng et al. 2015a, b; Wei et al. 2016; Yang et al. 2016a, b, 2017a, 2018; Yang and Zheng 2016; Zheng and Yang 2017; Yang and Zheng 2017) have been proposed to fulfill this task.

As a representative of discontinuous methods, the discontinuous deformation analysis (DDA) method (Shi 1988; Cheng and Zhang 2002; Zheng et al. 2017) is very suitable for modeling the mechanical behavior of a highly discrete rock block system. Note that the block system used in DDA analysis is generated by joint incision. How to establish a real three-dimensional (3D) rock block system is still a challenging task in DDA analysis (Chen et al. 2017; Jiang and Zhou 2017). Over the past three decades, DDA method has been extensively investigated and applied in solving many types of engineering problems such as tunnel engineering (Tsesarsky and Hatzor 2006; Zhu et al. 2016), slope engineering (Lin et al. 1996; Wu 2007), dam engineering (Dong et al. 1996; Kottenstette 1999), stability analysis of ancient masonry structures (Sasaki et al. 2011), rock hydraulic fracturing (Jiao et al. 2015; Choo et al. 2016), seismic response evaluation (Bao et al. 2013; Zhang et al. 2014), and rock burst analysis (Chen et al. 2018).

Up to now, many scholars have tried to improve the performance of the traditional DDA method by modifying the codes developed by Shi (Yu and Yin 2015). Ke (1995), MacLaughlin and Sitar (1996), Cheng and Zhang (2000), and Jiang and Zheng (2015) proposed different schemes to overcome false Vol. expansion of the DDA method when simulating large rotation problems. Lin et al. (1996) introduced artificial joints and subblocks into big blocks to simulate fracture in blocks. Hsiung (2001) replaced the first-order displacement function in the traditional DDA method with a higher-order displacement function, while Grayeli and Hatami (2008) adopted finite-element mesh to partition DDA blocks to obtain more accurate stress distribution. Apart from the penalty method, contacts between blocks are modeled by Cai et al. (2000) using a Lagrange multiplier method, by Lin et al. (1996) and Bao et al. (2014) using an augmented Lagrangian method (ALM), and by Zheng and Jiang (2009) and Zheng and Li (2015) using a complementary theory. Moreover, many efforts have been made to develop a 3D DDA method (Zhu et al. 2016; Yeung et al. 2003, 2007; Jiang and Yeung 2004; Beyabanaki et al. 2010). The biggest obstacle to thwart the 3D DDA method is the detection of contacts. In order to

[1]Assistant Professor, State Key Laboratory of Geomechanics and Geotechnical Engineering, Institute of Rock and Soil Mechanics, Chinese Academy of Sciences, Wuhan 430071, China (corresponding author). Email: scuhhc@126.com; ytyang@whrsm.ac.cn

[2]Associate Professor, Key Laboratory of Geotechnical Mechanics and Engineering, Ministry of Water Resources, Yangtze River Scientific Research Institute, Wuhan 430010, China. Email: xdhappy717@163.com

[3]Professor, Key Laboratory of Urban Security and Disaster Engineering, Ministry of Education, Beijing Univ. of Technology, Beijing 100124, China. Email: hzheng@whrsm.ac.cn

Note. This manuscript was submitted on October 13, 2017; approved on March 13, 2018; published online on June 20, 2018. Discussion period open until November 20, 2018; separate discussions must be submitted for individual papers. This paper is part of the ***International Journal of Geomechanics***, © ASCE, ISSN 1532-3641.

facilitate contact treatment of the 3D DDA method, Shi recently published a new contact theory (Shi 2015).

Note that the implicit time integration scheme is used to integrate equations of motion in the traditional DDA method. In each time step, the open–close (OC) iteration, which can be considered as a process of repeatedly adding or removing contact springs, is used to assure the correct arrangement of constraints. During OC iteration, global equations are constantly solved until each of contacts converges to a constant state (Mikola and Sitar 2013). If the convergence of contacts is not achieved within six iterations, the length of time step will be reduced and all related matrices including mass matrix, stiffness matrix, and load vector will be reassembled. Hence, the computational workload of the traditional DDA method is very heavy.

Moreover, the maximal allowable incremental displacement ($\triangle u^{\max}$) is specified by a user input value to ensure infinitesimal displacements. If the maximal incremental displacement $\triangle u$ is greater than $\triangle u^{\max}$, the length of time step will also be reduced and all related matrices should also be reassembled.

For small-scale problems with a small number of contact pairs, the traditional DDA method can use a relatively larger time step than the DEM. For large-scale problems with a great number of contact pairs, choosing a large time step is inappropriate; a large time-step value may cause large penetrations and more iterations are needed to satisfy the penetration threshold. Time-step cuts not only reduce the length of time step but also increase cumulative OC iterations (Mikola and Sitar 2013). Khan (2010) even concluded that although a larger time step can be specified in the DDA method, the real average time-step size is much smaller than that of the DEM with explicit time integration.

In order to reduce computational effort and memory requirement, Mikola and Sitar (2013) developed a DDA method using an explicit time integration scheme. Compared with the implicit time integration scheme, there is no need for the explicit time integration scheme to assemble a global mass and stiffness matrix. Therefore, solving large-scale simultaneous algebraic equations can be avoided.

In this study, formulations of an explicit DDA (EDDA) method proposed by Mikola and Sitar (2013) are further optimized. In Mikola and Sitar's formulations, a mass matrix for each DDA block is not lumped, and the inversion of all block mass matrices is inevitable. Here, each block mass matrix is a 6×6 submatrix for a 2D problem. To avoid the inversion of all block mass submatrices, a scheme to lump the mass matrix of each DDA block is proposed. The proposed EDDA method is more efficient than Mikola and Sitar's EDDA method, and much more efficient than the traditional DDA method for large-scale problems. The proposed EDDA method deserves to be further investigated for engineering computations in rock engineering. For the sake of illustration, only a 2D version of the proposed EDDA method is discussed in this paper. Note that the proposed EDDA method is different from the DEM proposed by Peter Cundall (Cundall 1971) since the "open–close iteration" and "simplex integration method" are used in the proposed EDDA method.

Fundamental Theory of the DDA Method

The DDA method (Shi 1988) is a numerical method for simulating the motion of a discrete rock block system. In the DDA method, large displacements and deformations are the accumulation of small displacements and small deformations of many time steps. Within each time step, displacements of all points are small and are taken incrementally.

Displacement Function of the DDA Method

Assuming each block has constant stresses and constant strains, the incremental displacements $(\Delta u, \Delta v)$ of any point (x, y) within a block can be represented through six degrees of freedom:

$$\{\Delta D_e\} = \{\Delta u_0 \quad \Delta v_0 \quad \Delta \gamma_0 \quad \Delta \varepsilon_x \quad \Delta \varepsilon_y \quad \Delta \gamma_{xy}\} \tag{1}$$

in which $(\Delta u_0, \Delta v_0)$ is the incremental rigid body translation of a specific point (x_0, y_0), typically the center of the block; $\Delta \gamma_0$ is the incremental rotation angle of the block, with the rotation center at (x_0, y_0). The unit of angle $\Delta \gamma_0$ is given in radians; $(\Delta \varepsilon_x, \Delta \varepsilon_y, \Delta \gamma_{xy})$ are incremental normal and shear strains of the block.

The incremental displacements of any point within this block can be expressed as

$$\begin{Bmatrix} \Delta u \\ \Delta v \end{Bmatrix} = [T_e]\{\Delta D_e\} \tag{2}$$

in which

$$[T_e] = \begin{Bmatrix} 1 & 0 & -(y-y_0) & (x-x_0) & 0 & (y-y_0)/2 \\ 0 & 1 & (x-x_0) & 0 & (y-y_0) & (x-x_0)/2 \end{Bmatrix} \tag{3}$$

Equations of Motion in a Discrete Form

Equations of motion in the DDA method can be expressed as (Doolin and Sitar 2004)

$$[M]\{\ddot{D}\} + [C]\{\dot{D}\} + [K(\{D\})]\{D\} = \{F(t, \{D\})\} \tag{4}$$

in which $[M]$, $[C]$, and $[K]$ are mass, damping, and stiffness matrices, respectively; and $F(t, \{D\})$ is a loading vector varying with time. The component forms for $[M]$, $[C]$, $[K]$, and $F(t, \{D\})$ have been presented in great detail by Shi (1988).

Let $\{D_n\}$ and $\{D_{n+1}\}$ respectively denote the approximation to values $\{D(t)\}$ and $\{D(t+h)\}$ for a time step h. Then, the discrete form for equations of motion [Eq. (4)] for a DDA system can be expressed as

$$[M]\{\ddot{D}_{n+1}\} + [C]\{\dot{D}_{n+1}\} + [K]\{D_{n+1}\} = \{F_{n+1}\} \tag{5}$$

with the initial conditions

$$\begin{cases} \{D(0)\} = \{0\} \\ \{\dot{D}(0)\} = \{\dot{D}_0\} \end{cases} \tag{6}$$

Solving Eq. (5) can adopt two methods including the direct integration method and the modal superposition method (Zienkiewicz and Taylor 2000). The scope of usage for these two methods has been discussed by Zienkiewicz and Taylor (2000). In the DDA method, the Newmark direct integration method is adopted.

According to the Newmark integration scheme of constant acceleration and let $\{D_n\} = \{0\}$, we have (Shi 1988)

$$\{D_{n+1}\} = h\{\dot{D}_n\} + \frac{h^2}{2}\{\ddot{D}_{n+1}\} \tag{7}$$

$$\{\dot{D}_{n+1}\} = \{\dot{D}_n\} + h\{\ddot{D}_{n+1}\} \tag{8}$$

Solving for $\{\ddot{D}_{n+1}\}$ from Eq. (7) leads to

$$\{\ddot{D}_{n+1}\} = \frac{2}{h^2}\{D_{n+1}\} - \frac{2}{h}\{\dot{D}_n\} \tag{9}$$

Substituting Eqs. (8) and (9) into Eq. (5) yields

$$[\widehat{K}]\{D_{n+1}\} = \{\widehat{F}\} \tag{10}$$

where $\{\widehat{K}\}$ is the general stiffness matrix, expressed as

$$[\widehat{K}] = \left(\frac{2}{h^2}[M] + \frac{2}{h}[C] + [K]\right) \tag{11}$$

and $\{\widehat{F}\}$ is the general loading vector, expressed as

$$\{\widehat{F}\} = \{F_{n+1}\} + \left(\frac{2}{h}[M] + [C]\right)\{\dot{D}_n\} \tag{12}$$

Note that the damping matrix $[C]$ is neglected in the traditional DDA method. The time integration scheme employed by the traditional DDA method contains inherent algorithmic damping (Doolin and Sitar 2004). Therefore, time-step size has a great influence on the accuracy and convergence rate of numerical solutions in the traditional DDA method (Jiang et al. 2013).

Due to the adoption of the updated Lagrange description to describe large displacements and deformations, configuration in the traditional DDA method is updated at the end of each time step. Therefore, $\{D_n\}$ is set as $\{0\}$ at the beginning of each time step. Obviously, $\{D_{n+1}\}$ in Eq. (10) are incremental displacements at the step $n+1$.

Due to the use of the implicit time integration scheme to integrate equations of motion, the traditional DDA method needs to assemble global mass and stiffness matrices. This requires that global equations be constantly solved. For large-scale problems under different loading conditions, the configuration of blocks will change with time, and some elements of the general global stiffness matrix may gradually move away from the diagonal. This will make solving the problem more time consuming and difficult.

Explicit Time Integration Scheme for the DDA Method

Compared with the implicit time integration scheme, the explicit time integration scheme can improve computational efficiency of large-scale problems. In the proposed EDDA method, an explicit forward central difference scheme is employed. This scheme can be modified by using the Verlet algorithm, in which velocity is calculated at each half time step (Langston et al. 1995). The Verlet algorithm can be expressed as (Qu et al. 2014)

$$\begin{cases} \{\dot{D}_{n+1/2}\} = \{\dot{D}_{n-1/2}\} + \{\ddot{D}_n\} \cdot h \\ \{\dot{D}_{n+1}\} = \{\dot{D}_{n+1/2}\} + \frac{1}{2}\{\ddot{D}_n\} \cdot h \\ \{D_{n+1}\} = \{D_n\} + \{\dot{D}_{n+1/2}\} \cdot h \end{cases} \tag{13}$$

Substituting Eq. (13) into Eq. (5) yields

$$[M]\{\ddot{D}_{n+1}\} = \{\bar{F}\} \tag{14}$$

where

$$\{\bar{F}\} = \{F_{n+1}\} - \{F_D\} - \{F_I\} \tag{15}$$

where $\{F_D\} = [C]\{\dot{D}_{n+1}\}$ is the damping term and the direction is such that the energy is always dissipated. $\{F_I\}$ is the internal force vector.

Lumped Mass Matrix

The mass matrix in Eq. (14) is normally called the global consistent mass matrix. As in FEM, the global consistent mass matrix in the DDA method can be easily obtained by assembling all block-consistent mass matrices. The block-consistent mass matrix for a given block e can be expressed as

$$[M_e] = \iint_A \left[T_e(x,y)\right]^T \rho \left[T_e(x,y)\right] dxdy \tag{16}$$

where $\left[T_e(x,y)\right]$ has been defined in Eq. (3).

In the FEM, based on the elemental consistent mass matrix (similar to the block-consistent mass matrix in the DDA method), the row-sum lumping technique (Zhu 2009) is often used to obtain the lumped mass matrix for low-order elements.

As discussed by Shi (1988) and Chen et al. (2001), the block displacement function in the traditional DDA method is equivalent to a complete first-order displacement approximation function. Therefore, row-sum lumping technique should also apply to the DDA method. However, according our test, the row-sum lumping technique fails in the DDA method. This may be because rotation angle and strains are treated as degrees of freedom in the traditional DDA method, and negative elements may not only exist in $[T_e]$ [Eq. (3)] but also exist in $[M_e]$ [Eq. (16)]. Therefore, if the row-sum lumping technique is applied on $[M_e]$, the resulting lumped mass matrix ($\left[\tilde{M}_e\right]$) of a block may have negative elements, which do not conform to an actual physical meaning.

If $[T_e]$ is replaced with a matrix $\left[\tilde{T}_e\right]$ in which all terms are nonnegative, then the resulting lumped matrix $\left[\tilde{M}_e\right]$ will not have negative terms. Therefore, we rewrite the DDA block displacement function in the following form (Chen et al. 2001):

$$u(x,y) = a_1 + a_2x + a_3y, \;\; v(x,y) = b_1 + b_2x + b_3y \tag{17}$$

where a_k and b_k ($k = 1, 2, 3$) are parameters yet to be determined.

In NMM (Zheng and Xu 2014), displacements (u, v) of any point (x,y) within a manifold element can be obtained by multiplying all weight functions $w_k(x,y)$ with local approximation functions $\boldsymbol{u}_k(x,y)$ and expressed as

$$\boldsymbol{u}(x,y) = \sum_{k=1}^{n^p} w_k(x,y)\boldsymbol{u}_k(x,y), \;\; (x,y) \in E_i \tag{18}$$

where n^p is the number of physical patches associated with manifold element E_i.

If triangular mesh is adopted to construct the mathematical mesh, and the shape function of constant strain triangular element is employed to construct weight functions, and constant parameters are employed to construct local approximation functions, the displacement function of NMM would be identical to Eq. (17).

Based on the above discussion, a DDA block can be considered as a manifold element. In other words, DDA is a spatial case of NMM. Fig. 1 shows a DDA block (or a manifold element) covered by an equilateral triangle mesh. The complete first-order displacement in incremental form within a manifold element can be expressed as

$$\begin{Bmatrix} \Delta u \\ \Delta v \end{Bmatrix} = \left[\tilde{T}_e\right]\{\Delta\tilde{D}_e\} \tag{19}$$

in which

$$[\tilde{T}_e] = \begin{Bmatrix} w_1 & 0 & w_2 & 0 & w_3 & 0 \\ 0 & w_1 & 0 & w_2 & 0 & w_3 \end{Bmatrix} \tag{20}$$

and

$$[\Delta\tilde{D}_e] = \{u_1 \quad v_1 \quad u_2 \quad v_2 \quad u_3 \quad u_3\}^{\mathrm{T}} \tag{21}$$

The weight function $w_i(\boldsymbol{x})$ is expressed as

$$w_1(\boldsymbol{x}) = L_1, \quad w_2(\boldsymbol{x}) = L_2, \quad w_3(\boldsymbol{x}) = L_3 \tag{22}$$

where L_i is the area coordinate (Zienkiewicz and Taylor 2000). In Fig. 1, the value of L_i would always be nonnegative. Note that the value of L_i is identical to the shape function of a three-node triangular element.

The new formulation of a consistent block mass matrix for a given block e is then expressed as

$$[M_e] = \iint_A \left[\tilde{T}_e(x,y)\right]^{\mathrm{T}} \rho \left[\tilde{T}_e(x,y)\right] dxdy \tag{23}$$

Since the value of L_i would always be nonnegative, there would be no negative terms in $[M_e]$ [Eq. (23)]. The row-sum lumping technique can now be applied on $[M_e]$ [Eq. (23)] to obtain a rational lumped block mass matrix $[\tilde{M}_e]$.

In the proposed EDDA method, each variable in $\{\ddot{D}_{n+1}\}$ is independent of other variables in $\{\ddot{D}_{n+1}\}$, and can be solved independently in each time step. In other words, there is no need to use any equation solver to solve Eq. (14), and the need to solve a complete system of equations can be totally avoided. There is also no need for the proposed EDDA method to assemble global mass and stiffness matrices.

Internal Force

Internal force $\{F_I\}$ in Eq. (15) can be calculated by a block stiffness matrix $[K^e]$. In a continuous problem, each block internal force $\{F_I^e\}$ is generated by $[K^e]$, which satisfies the equations of motion:

$$[M^e]\{\ddot{D}_{n+1}\} = \{\bar{F}^e\} \tag{24}$$

$$\{\bar{F}^e\} = \{F_{n+1}^e\} - \{F_D^e\} - \{F_I^e\} \tag{25}$$

For a discontinuous deformation analysis problem, $[K^e]$ includes two parts, namely, the block stiffness matrix $[\tilde{K}^e]$ and the contact matrix $[\tilde{K}^c]$.

$$[K^e] = [\tilde{K}^e] + [\tilde{K}^c] \tag{26}$$

Therefore, the internal force can be expressed as

$$\{F_I^e\} = [K^e]\{D_{n+1}\} = \left([\tilde{K}^e] + [\tilde{K}^c]\right)\{D_{n+1}\} \tag{27}$$

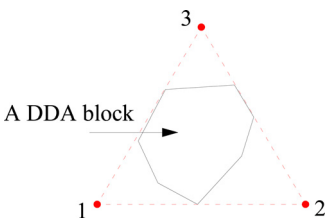

Fig. 1. A DDA block covered by an equilateral triangular mesh.

For a discrete block system, assuming a contact pair exists between block i and j, the contact stiffness matrix $[Q]$ corresponding to this contact pair can be expressed as

$$[Q] = \begin{bmatrix} \tilde{K}_{ii}^c & \tilde{K}_{ij}^c \\ \tilde{K}_{ji}^c & \tilde{K}_{jj}^c \end{bmatrix} \tag{28}$$

in which $\left[\tilde{K}_{ij}^c\right]$ is defined by the contact spring between contact blocks i and j. The value of $\left[\tilde{K}_{ij}^c\right]$ is zero if blocks i and j have no contact. The matrix $\left[\tilde{K}_{ij}^c\right]$ is a 6×6 submatrix and the formulation of $\left[\tilde{K}_{ij}^c\right]$ will be discussed in detail in the following content. The vector $\{D_{n+1}\}$ can be calculated by Eq. (13).

Apart from the contact stiffness matrix, a contact spring will also bring in a submatrix of contact force, and the friction force will produce the corresponding submatrix of frictional force, which will all be added into the loading vector $\{\bar{F}\}$.

In the DDA method, there are two types of contact springs: the normal contact spring, and the tangential contact spring. Calculating the normal spring stiffness matrix, the tangential stiffness matrix, and the corresponding subvectors of contact force will yield different $[\tilde{K}^c]$, $\{F_i^c\}$, and $\{F_j^c\}$.

Submatrix for a Normal Contact Spring

Assuming P_1 is a vertex, P_2P_3 is the entrance line. Then (x_k, y_k) and (uk, vk) are coordinates and displacements of P_k (k = 0, 1, 2, 3), respectively (Fig. 2).

Based on the principle of minimum potential energy, four sets of 6×6 submatrices, namely, $\left[\tilde{K}_{ii}^c\right]$, $\left[\tilde{K}_{ij}^c\right]$, $\left[\tilde{K}_{ji}^c\right]$, and $\left[\tilde{K}_{jj}^c\right]$, and two sets of 6×1 subvectors, namely, $\{F_i^c\}$ and $\{F_j^c\}$, can be obtained for a normal contact spring. Expressions for submatrices and subvectors related to normal spring are presented as follows (Shi 1991):

$$\begin{cases} \left[\tilde{K}_{ii}^c\right] = p_n\{H\}\{H\}^{\mathrm{T}} \\ \left[\tilde{K}_{ij}^c\right] = p_n\{G\}\{H\}^{\mathrm{T}} \\ \left[\tilde{K}_{ji}^c\right] = p_n\{H\}\{G\}^{\mathrm{T}} \\ \left[\tilde{K}_{jj}^c\right] = p_n\{G\}\{G\}^{\mathrm{T}} \end{cases} \tag{29}$$

$$\begin{cases} \{F_i^c\} = -\dfrac{p_n S_0\{H\}}{l} \\ \{F_j^c\} = -\dfrac{p_n S_0\{G\}}{l} \end{cases} \tag{30}$$

where p_n is the stiffness of the normal contact spring,

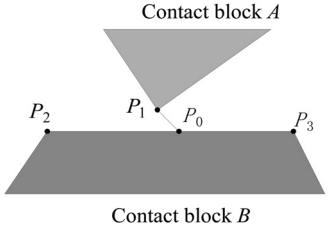

Fig. 2. Contact model.

$$\begin{cases} \{H\} = \dfrac{1}{l}\left[\tilde{T}_i(x_1, y_1)\right]^{\mathrm{T}} \begin{Bmatrix} y_2 - y_3 \\ x_3 - x_2 \end{Bmatrix} \\ \{G\} = \dfrac{1}{l}\left[\tilde{T}_j(x_2, y_2)\right]^{\mathrm{T}} \begin{Bmatrix} y_3 - y_1 \\ x_1 - x_3 \end{Bmatrix} \\ + \dfrac{1}{l}\left[\tilde{T}_j(x_3, y_3)\right]^{\mathrm{T}} \begin{Bmatrix} y_1 - y_2 \\ x_2 - x_1 \end{Bmatrix} \end{cases} \tag{31}$$

and

$$S_0 = \begin{vmatrix} 1 & x_1 & y_1 \\ 1 & x_2 & y_2 \\ 1 & x_3 & y_3 \end{vmatrix} \tag{32}$$

Submatrix for a Tangential Contact Spring

Similar to the normal contact spring, and based on the principle of minimum potential energy, four sets of 6×6 submatrices, namely, $\left[\tilde{K}_{ii}^c\right]$, $\left[\tilde{K}_{ij}^c\right]$, $\left[\tilde{K}_{ji}^c\right]$, and $\left[\tilde{K}_{jj}^c\right]$, and two sets of 6×1 subvectors, namely, $\{F_i^c\}$, and $\{F_j^c\}$, can also be obtained for a tangential contact spring. Expressions for submatrices and subvectors associated with the tangential contact spring are as follows (Shi 1991):

$$\begin{cases} \left[\tilde{K}_{ii}^c\right] = p_\tau \{H\}\{H\}^{\mathrm{T}} \\ \left[\tilde{K}_{ij}^c\right] = p_\tau \{G\}\{H\}^{\mathrm{T}} \\ \left[\tilde{K}_{ji}^c\right] = p_\tau \{H\}\{G\}^{\mathrm{T}} \\ \left[\tilde{K}_{jj}^c\right] = p_\tau \{G\}\{G\}^{\mathrm{T}} \end{cases} \tag{33}$$

$$\begin{cases} \{F_i^c\} = -\dfrac{p_\tau S_0 \{H\}}{l} \\ \{F_j^c\} = -\dfrac{p_\tau S_0 \{G\}}{l} \end{cases} \tag{34}$$

where p_τ is the stiffness of the tangential contact spring,

$$\begin{cases} \{H\} = \dfrac{1}{l}\left[\tilde{T}_i(x_1, y_1)\right]^{\mathrm{T}} \begin{Bmatrix} x_3 - x_2 \\ y_3 - y_2 \end{Bmatrix} \\ \{G\} = \dfrac{1}{l}\left[\tilde{T}_j(x_0, y_0)\right]^{\mathrm{T}} \begin{Bmatrix} x_2 - x_3 \\ y_2 - y_3 \end{Bmatrix} \end{cases} \tag{35}$$

and

$$S_0 = (x_1 - x_0)(x_3 - x_2) + (y_1 - y_0)(y_3 - y_2) \tag{36}$$

Submatrix for Friction Force

The friction force is calculated from the normal contact compressive force, and the direction of the friction force depends on the movement of P_1 relative to P_0 in the direction from P_2 to P_3. Let p_n be stiffness of the normal contact spring, then the friction force can be obtained through Eq. (37):

$$F_0 = p_n \cdot d_n \cdot \mathrm{sgn}(d_r) \cdot \tan(\varphi) \tag{37}$$

where d_n is the normal penetration distance; φ is the friction angle; $\tan(\varphi)$ is the friction coefficient; d_r is the movement of P_1 relative to P_0 in the direction from P_2 to P_3; and sgn is a symbolic function defined as

$$\mathrm{sgn}(x) = \begin{cases} 1, & \text{if } x > 0, \\ 0, & \text{if } x = 0, \\ -1, & \text{if } x < 0. \end{cases} \tag{38}$$

Subvectors for the friction force can then be expressed as (Shi 1991)

$$\begin{cases} \{F_i^c\} = -F_0\{H\} \\ \{F_j^c\} = F_0\{G\} \end{cases} \tag{39}$$

where

$$\begin{cases} \{H\} = \dfrac{1}{l}\left[\tilde{T}_i(x_1, y_1)\right]^{\mathrm{T}} \begin{Bmatrix} x_3 - x_2 \\ y_3 - y_2 \end{Bmatrix} \\ \{G\} = \dfrac{1}{l}\left[\tilde{T}_j(x_0, y_0)\right]^{\mathrm{T}} \begin{Bmatrix} x_3 - x_2 \\ y_3 - y_2 \end{Bmatrix} \end{cases} \tag{40}$$

OC Iteration

In the traditional DDA method, a penalty method is adopted to deal with contact problems. The penalty method is incorporated into the DDA method by adding contact springs to produce contact stiffness matrices and force vectors and then assembling them into global equations to obtain incremental displacements of each time step. There are three types of contacts in DDA method: vertex–vertex, vertex–edge, and edge–edge. Each contact pair may have one (only normal) or two (both normal and tangential) contact springs. To ensure the correct arrangement of contact springs, the OC iteration technique is used in the DDA method. During the process of OC iteration, global equations are constantly solved until each of contacts converges to a constant state within a time step (Mikola and Sitar 2013). If contact convergence is not achieved within six iterations, the length of the time step will be reduced and the analysis will be repeated with this reduced time step. Additionally, the maximal allowable incremental displacement $\triangle u^{\max}$ is specified by a user input value to ensure infinitesimal displacements. If the maximal incremental displacement is greater than $\triangle u^{\max}$, the length of the time step will also be reduced and the analysis will also be repeated. As expected, in dealing with discontinuous problems with a large number of contact pairs, the number of OC iterations will be significantly increased and the process will become increasingly time consuming.

Since the length of time step in the proposed EDDA method is relatively small, OC iteration can converge in one time step. More importantly, due to the adoption of lumped mass matrix, there is no need to assemble global mass and stiffness matrices. Hence, the proposed EDDA method is very efficient in terms of solving equations, even with the OC iteration involved.

The explicit time integration scheme is conditionally stable, that is, the time-step size must be smaller than a certain critical value (i.e., critical time step, Δt_c) for numerical errors not to grow unbounded (Mikola and Sitar 2013). The time increment must satisfy the well-known criterion presented in Eq. (41):

$$\Delta t = \frac{2}{\omega_{\max}} \tag{41}$$

where $\omega_{\max}$ is the maximum element eigenvalue.

The damping in the DDA method has already been studied by Jiang et al. (2013), hence we will not discuss damping in this study.

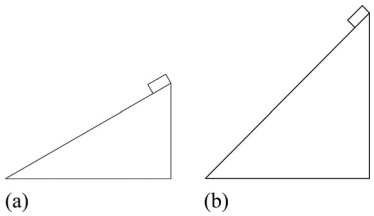

Fig. 3. Block slides along a ramp: (a) slope angle α = 30°; and (b) slope angle α = 45°.

Integration

In the traditional DDA method, the simplex integration method is normally employed to carry out integration. By using the simplex integration method, exact integration over an arbitrarily shaped block can be carried out without difficulty and no extra consideration is needed. The element partitioning scheme, which is often used in other methods, such as in the extended finite-element method (XFEM) (Fries and Belytschko 2010) to conduct numerical integration, is totally unnecessary in the DDA method. Therefore, the simplex integration method will be used in the proposed EDDA method.

Numerical Examples

Typical numerical tests solved with the proposed EDDA method were carried out, and the results are compared with those of the traditional DDA method. The physical units used in the present work are based on the International System of Units (SI) without specification.

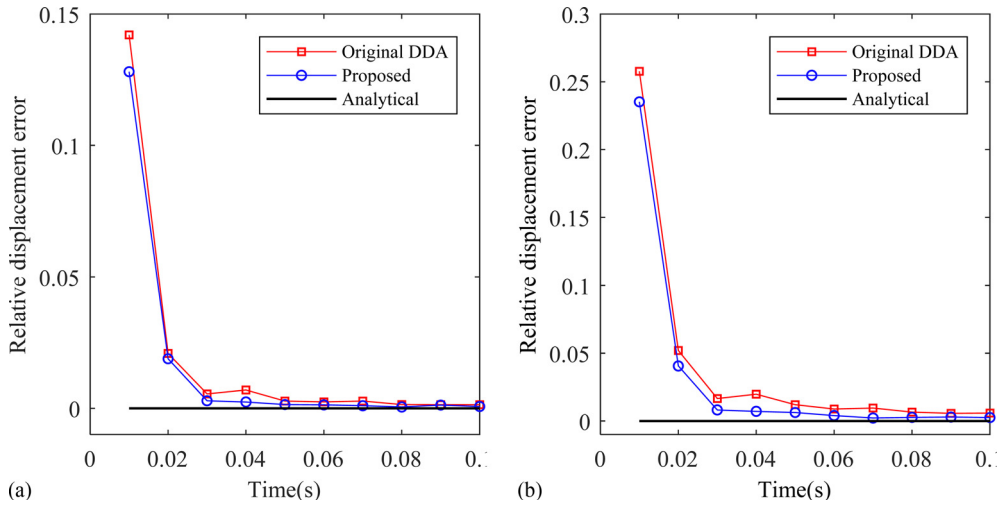

Fig. 4. Comparisons between the proposed EDDA method and the traditional DDA method under slope angles α = 30° and different friction angles: (a) ϕ = 10°; and (b) ϕ = 15°.

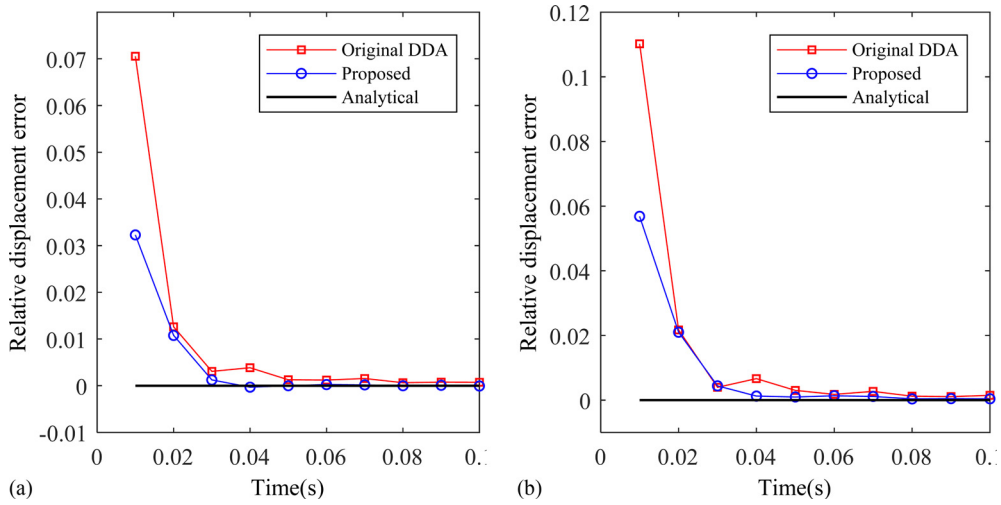

Fig. 5. Comparisons between the proposed EDDA method and the traditional DDA method under slope angles α = 45° and different friction angles: (a) ϕ = 10°; and (b) ϕ = 15°.

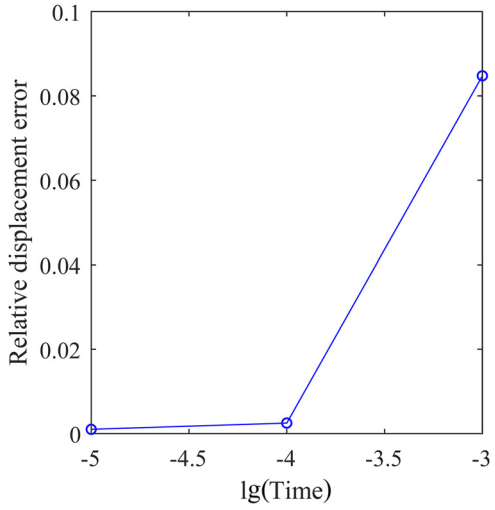

Fig. 6. Influence of time-step length on accuracy of the proposed EDDA method (slope angle $\alpha = 30°$, friction angle $\phi = 15°$).

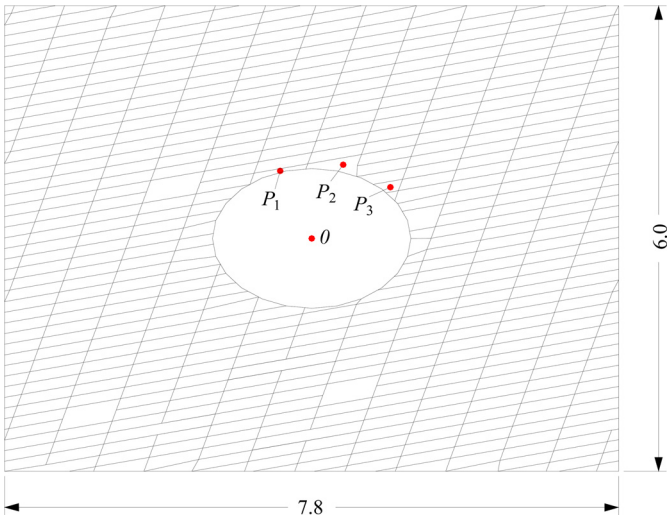

Fig. 7. Underground cavern intersected by two sets of joints. (Reprinted with permission from Shi 1988.)

Sliding Problem

Using this classical example, accuracy obtained through the proposed EDDA method is compared with that obtained through the traditional DDA method. Fig. 3 shows a sliding rectangle block with dimensions 2×1 m on a ramp with a slope angle of α. The block and the ramp have the same material parameters: Young's modulus E = 200 MPa; Poisson's ratioν = 0.25; and density ρ = 2,750 kg/m^3. Bottom and right sides of the ramp are all fixed by stiff springs with a stiffness of 1,000E in both horizontal and vertical directions.

It is easy to derive the exact sliding displacement of the block:

$$s = \frac{1}{2}(\sin\alpha - \mu\cos\alpha)gt^2 \tag{42}$$

at time t (s), where s = sliding distance of the block center point (m); g = gravity speed (9.8 m/s^2); $\mu = \tan\phi$; and ϕ = friction angle.

Let the length of time step (Δt) = 1×10^{-4}s and the total computation time = 0.1 s, with a set of combinations of slope angles and friction angles assumed. Figs. 4 and 5 display the relative error distributions obtained from the proposed EDDA and traditional DDA methods during sliding. The results obtained through the proposed EDDA method are slightly better than those obtained through the traditional DDA method.

To study the effect of the length of time step on the accuracy of the solution obtained through the proposed EDDA method, three types of time-step lengths ($\Delta t = 1 \times 10^{-5}$ s, 1×10^{-4} s, and 1×10^{-3} s) were tested. In this example, only the case with the slope angle α = 30° and the friction angle ϕ = 15° was investigated. Fig. 6 displays the relative error distributions obtained through the proposed EDDA method. The accuracy obtained through the proposed EDDA method becomes better and better as the length of time step decreases.

Underground Cavern

As shown in Fig. 7, a cavern built in the stratum cut by two sets of joints (Shi 1988) is simulated by both the traditional DDA method and the proposed EDDA method. Material parameters are assumed as follows: Young's modulus E = 19 GPa; Poisson's ratio ν = 0.25; density ρ = 2,630 kg/m^3; and unit weight γ = 26,300 N/m^3. Input parameters for the computation are stiffness of contact springs g0 = 190 GPa; length of time step g1 = 1×10^{-7}s; and ratio of maximum displacement g2 = 5×10^{-6}. Cohesion and friction angle of contact surfaces are assumed to be 0° and 5°, respectively. The bottom, top, left, and right sides of the model are all fixed by stiff springs with a stiffness of 1,000E in both horizontal and vertical directions.

Fig. 8 displays displacements of monitoring points calculated by the proposed EDDA and traditional DDA methods. As can be seen in Fig. 8, results obtained through the proposed EDDA method agree well with those obtained through the traditional DDA method.

Discussion and Conclusions

Based on the explicit time integration scheme, an explicit version of the DDA (EDDA) method is proposed to reduce the computational effort and memory requirement. Due to the numerical stability, a smaller time-step length is needed in the proposed EDDA method than in the traditional DDA method. However, the process of assembling global stiffness and mass matrices can be avoided in the proposed EDDA method. Hence, the memory requirement can be significantly reduced. More importantly, the proposed EDDA method can avoid solving simultaneous algebraic equations. Numerical tests conducted in this paper show that accuracy obtained through the proposed EDDA method is slightly better than that obtained through the traditional DDA method (Figs. 4 and 5).

Compared with the EDDA method proposed by Mikola and Sitar (2013), the global mass matrix in the proposed EDDA method is lumped and the computational effort and memory requirement are further reduced.

Compared with the OC iteration used in the traditional DDA method, the OC iteration in the proposed EDDA method is more efficient in terms of convergence. This is because solving simultaneous algebraic equations can be avoided in the proposed EDDA method at each iteration. In addition, a smaller penetration is incurred due to a smaller time-step length being used.

Additionally, the simplex integration method, which is capable of conducting exact integration over an arbitrarily shaped block, is employed in the proposed EDDA method.

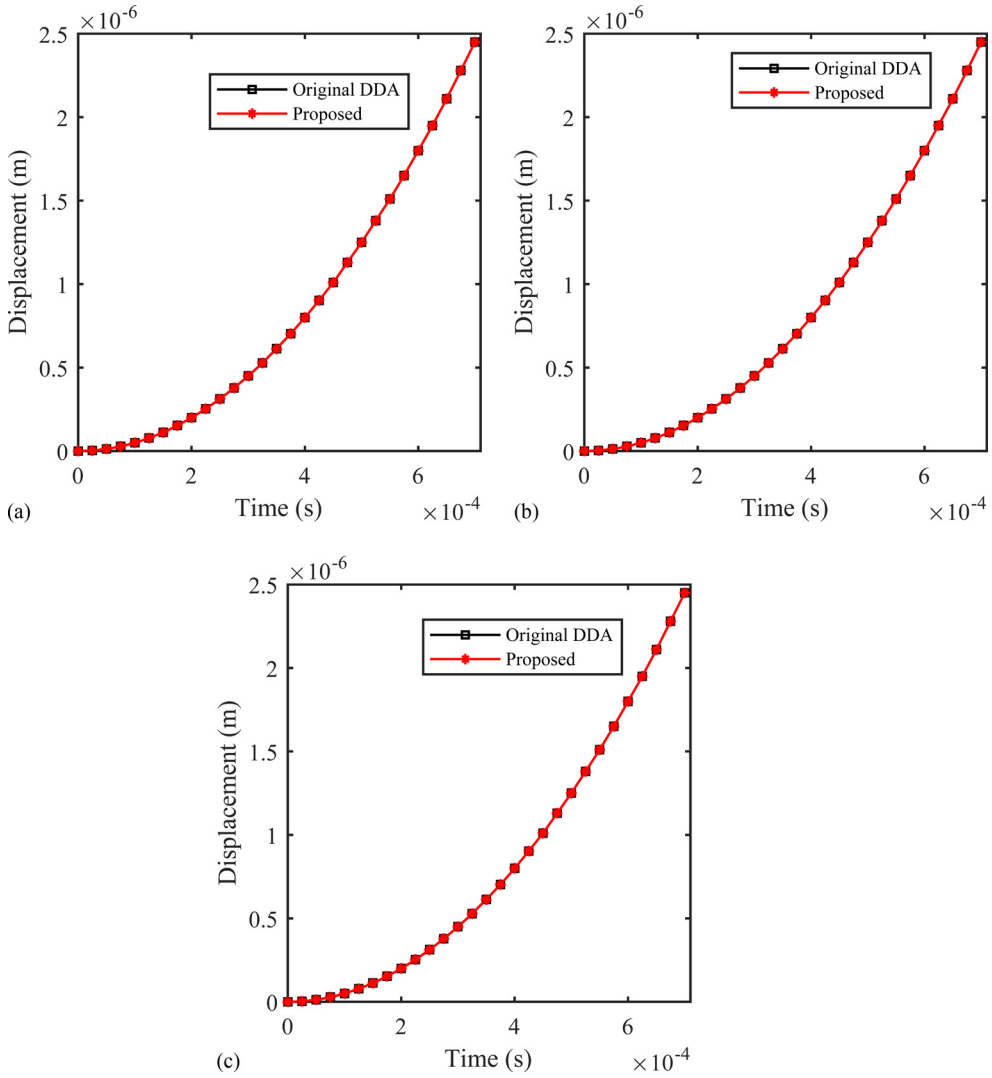

Fig. 8. Displacements of the monitoring points calculated by the proposed EDDA method and the traditional DDA method: (a) displacements of P_1; (b) displacements of P_2; and (c) displacements of P_3.

In view of the above characteristics, the proposed EDDA method is more suitable for solving large-scale problems, and it is worth further investigation for engineering computations in rock engineering. However, real rock mechanics problems are in three dimensions. Extension of the proposed 2D EDDA method to the 3D EDDA method is essential. In a future study, we will develop a 3D EDDA method to solve real rock mechanics problems.

Acknowledgments

This study was supported by the National Natural Science Foundation of China, under Grant 51609240, 11172313, and 51538001, and by the National Basic Research Program of China (973 Program), under Grant 2014CB047100.

References

Antolini, F., M. Barla, G. Gigli, and A. Giorgetti. 2016. "Combined finite–discrete numerical modeling of runout of the Torgiovannetto di Assisi rockslide in central Italy." *Int. J. Geomech.* 16 (6): 04016019. https://doi.org/10.1061/(ASCE)GM.1943-5622.0000646.

Bao, H. R., G. Yagoda-Biran, and Y. H. Hatzor. 2013. "Site response analysis with two-dimensional numerical discontinuous deformation analysis method." *Earthquake Eng. Struct. Dyn.* 43 (2): 225–246. https://doi.org/10.1002/eqe.2340.

Bao, H. R., Z. Y. Zhao, and Q. Tian. 2014. "On the implementation of augmented Lagrangian method in the two-dimensional discontinuous deformation analysis." *Int. J. Numer. Anal. Meth. Geomech.* 38 (6): 551–571. https://doi.org/10.1002/nag.2217.

Barla, M., G. Piovano, and G. Grasselli. 2012. "Rock slide simulation with the combined finite-discrete element method." *Int. J. Geomech.* 12 (6): 711–721. https://doi.org/10.1061/(ASCE)GM.1943-5622.0000204.

Beskos, D. E. 1997. "Boundary element methods in dynamic analysis: Part II (1986–1996)." *Appl. Mech. Rev.* 50 (3): 149–197. https://doi.org/10.1115/1.3101695.

Beyabanaki, S., A. Jafari, and M. R. Yeung. 2010. "High-order three-dimensional discontinuous deformation analysis (3-D DDA)." *Int. J. Numer. Meth. Bio.* 26 (12): 1522–1547.

Cai, Y. G., T. He, and R. Wang. 2000. "Numerical simulation of dynamic process of the Tangshan Earthquake by a new method—LDDA." *Pure. Appl. Geophys.* 157 (11–12): 2083–2104. https://doi.org/10.1007/PL00001076.

Chen, G., M. He, and F. Fan. 2018. "Rock burst analysis using DDA numerical simulation." *Int. J. Geomech.* 18 (3): 04018001. https://doi.org/10.1061/(ASCE)GM.1943-5622.0001055.

Chen, G. Q., K. Zen, Y. Ohnishi, and K. Kasama. 2001. "Extension of manifold method and its application." In *Proc., 4th International Conf. on Analysis of Discontinuous Deformation (ICADD-4)*, edited by N. Bićanić, 439–450. Glasgow, UK: International Conference on Analysis of Discontinuous Deformation.

Chen, N., J. Kemeny, Q. H. Jiang, and Z. W. Pan. 2017. "Automatic extraction of blocks from 3D point clouds of fractured rock." *Comput. Geosci.* 109: 149–161. https://doi.org/10.1016/j.cageo.2017.08.013.

Cheng, Y. M., and Y. H. Zhang. 2000. "Rigid body rotation and block internal discretization in DDA analysis." *Int. J. Numer. Anal. Meth. Geomech.* 24 (6): 567–578. https://doi.org/10.1002/(SICI)1096-9853(200005)24:6<567::AID-NAG83>3.0.CO;2-N.

Cheng, Y. M., and Y. H. Zhang. 2002. "Coupling of FEM and DDA Methods." *Int. J. Geomech.* 2 (4): 503–517. https://doi.org/10.1061/(ASCE)1532-3641(2002)2:4(503).

Choo, L. Q., Z. Zhao, H. Chen, and Q. Tian. 2016. "Hydraulic fracturing modeling using the discontinuous deformation analysis (DDA) method." *Comput. Geotech.* 76: 12–22. https://doi.org/10.1016/j.compgeo.2016.02.011.

Cundall, P. A. 1971. "A computer model for simulating progressive, large-scale movements in blocky rock systems." In Vol. 1 of *Proc., Symp. of the Int. Society of Rock Mechanics*, 1–8. Nancy, France: International Society of Rock Mechanics.

Desai, C. S., M. M. Zaman, J. G. Lightner, and H. J. Siriwardane. 1984. "Thin-layer element for interfaces and joints." *Int. J. Numer. Anal. Meth. Geomech.* 8 (1): 19–43. https://doi.org/10.1002/nag.1610080103.

Dong, X., A. Wu, and F. Ren. 1996. "A preliminary application of discontinuous deformation analysis (DDA) to the Three Gorges Dam project." In *Proc., First Int. Forum on Discontinuous Deformation Analysis (DDA) and Simulations of Discontinuous Media*, edited by M. R. Salami, and D. Banks, 310–317. Albuquerque, NM: TSI Press.

Doolin, D. M., and N. Sitar. 2004. "Time integration in discontinuous deformation analysis." *J. Eng. Mech.* 130 (3): 249–258. https://doi.org/10.1061/(ASCE)0733-9399(2004)130:3(249).

Elmo, D., D. Stead, E. Eberhardt, and A. Vyazmensky. 2013. "Applications of finite/discrete element modeling to rock engineering problems." *Int. J. Geomech.* 13 (5): 565–580. https://doi.org/10.1061/(ASCE)GM.1943-5622.0000238.

Fan, L. F., X. W. Yi, and G. W. Ma. 2013. "Numerical manifold method (NMM) simulation of stress wave propagation through fractured rock mass." *Int. J. Appl. Mech.* 5 (2): 1350022. https://doi.org/10.1142/S1758825113500221.

Fries, T. P., and T. Belytschko. 2010. "The extended/generalized finite element method: An overview of the method and its applications." *Int. J. Numer. Methods. Eng.* 84 (3): 253–304.

Goodman, R. E., and St. John. 1977. "Chapter 4: Finite element analysis for discontinuous rocks." In *Numerical methods in geotechnical engineering*, edited by C. S. Desai and J. T. Christian, 148–175. New York: McGraw-Hill Book Company.

Grayeli, R., and K. Hatami. 2008. "Implementation of the finite element method in the three-dimensional discontinuous deformation analysis (3D-DDA)." *Int. J. Numer. Anal. Meth. Geomech.* 32 (15): 1883–1902. https://doi.org/10.1002/nag.704.

Hsiung, S. M. 2001. "Discontinuous deformation analysis (DDA) with nth order polynomial displacement functions." In *Proc., 38th US Rock Mechanics Symp.: Rock Mechanics in the National Interest*, edited by D. Elsworth, J. P. Tinucci, and K. A. Heasley, 1413–1420. Washington, DC: American Rock Mechanics Association.

Jiang, Q. H., Y. F. Chen, C. B. Zhou, and M. R. Yeung. 2013. "Kinetic energy dissipation and convergence criterion of discontinuous deformations analysis (DDA) for geotechnical engineering." *Rock Mech. Rock Eng.* 46 (6): 1443–1460. https://doi.org/10.1007/s00603-012-0356-5.

Jiang, Q. H., and M. R. Yeung. 2004. "A model of point-to-face contact for three-dimensional discontinuous deformation analysis." *Rock Mech. Rock Eng.* 37 (2): 95–116. https://doi.org/10.1007/s00603-003-0008-x.

Jiang, Q. H., and C. B. Zhou. 2017. "A rigorous solution for the stability of polyhedral rock blocks." *Comput. Geotech.* 90: 190–201. https://doi.org/10.1016/j.compgeo.2017.06.012.

Jiang, W., and H. Zheng. 2015. "An efficient remedy for the false volume expansion of DDA when simulating large rotation." *Comput. Geotech.* 70: 18–23. https://doi.org/10.1016/j.compgeo.2015.07.008.

Jiao, Y. Y., H. Q. Zhang, X. L. Zhang, H. B. Li, and Q. H. Jiang. 2015. "A two-dimensional coupled hydromechanical discontinuum model for simulating rock hydraulic fracturing." *Int. J. Numer. Anal. Meth. Geomech.* 39 (5): 457–481. https://doi.org/10.1002/nag.2314.

Katona, M. G. 1983. "A simple contact–friction interface element with applications to buried culverts." *Int. J. Numer. Anal. Meth. Geomech.* 7 (3): 371–384. https://doi.org/10.1002/nag.1610070308.

Ke, T. C. 1995. "Modification of DDA with respect to rigid body rotation." In *Proc., 1st Int. Conf. on Analysis of Discontinuous Deformation*, edited by J. C. Li, C. Y. Wang, and J. Sheng, 260–273. Chungli, Taiwan, China: National Central Univ.

Khan, M. S. 2010. "Investigation of discontinuous deformation analysis for application in jointed rock masses." Ph.D. thesis, Department of Civil Engineering, Univ. of Toronto.

Kottenstette, J. T. 1999. "DDA analysis of the RCC modification for Pueblo Dam." In *Proc., ICADD-3: Third Int. Conf. on Analysis of Discontinuous Deformation-From Theory to Practice*, edited by B. Amadei, 127–132. Washington DC: American Rock Mechanics Association, Balkema.

Langston, P. A., U. Tüzün, and D. M. Heyes. 1995. "Discrete element simulation of granular flow in 2D and 3D hoppers: Dependence of discharge rate and wall stress on particle interactions." *Chem. Eng. Sci.* 50 (6): 967–987. https://doi.org/10.1016/0009-2509(94)00467-6.

Lin, C. T., B. Amadei, J. Jung, and J. Dwyer. 1996. "Extensions of discontinuous deformation analysis for jointed rock masses." *Int. J. Rock Mech. Min. Sci. Geomech. Abstr.* 33 (7): 671–694. https://doi.org/10.1016/0148-9062(96)00016-2.

Ma, G., W. Zhou, X. L. Chang, and W. Yuan. 2014. "Combined FEM/DEM modeling of triaxial compression tests for rockfills with polyhedral particles." *Int. J. Geomech.* 14 (4): 04014014. https://doi.org/10.1061/(ASCE)GM.1943-5622.0000372.

MacLaughlin, M. M., and N. Sitar. 1996. "Rigid body rotations in DDA." In *Proc., 1st Int. Forum on DDA and Simulations of Discontinuous Media*, edited by M. R. Salami, and D. Banks, 620–636. Berkeley, CA: TSI Press.

Mahabadi, O. K., A. Lisjak, A. Munjiza, and G. Grasselli. 2012. "Y-Geo: New combined finite-discrete element numerical code for geomechanical applications." *Int. J. Geomech.* 12 (6): 676–688. https://doi.org/10.1061/(ASCE)GM.1943-5622.0000216.

Mikola, R. G., and N. Sitar. 2013. "Explicit three dimensional discontinuous deformation analysis for blocky system." In *Proc., 47th US Rock Mechanics/Geomechanics Symp. 2013*, edited by L. J. Pyrak-Nolte, A. Chan, W. Dershowitz J. Morris, and J. Rostami, 1320–1327. San Francisco: American Rock Mechanics Association.

Munjiza, A. 2004. *The combined finite-discrete element method.* Hoboken, NJ: John Wiley & Sons.

Ning, Y. J., X. M. An, and G. W. Ma. 2011. "Footwall slope stability analysis with the numerical manifold method." *Int. J. Rock Mech. Min. Sci.* 48 (6): 964–975. https://doi.org/10.1016/j.ijrmms.2011.06.011.

Qu, X. L., G. Y. Fu, and G. W. Ma. 2014. "An explicit time integration scheme of numerical manifold method." *Eng. Anal. Bound. Elem.* 48: 53–62. https://doi.org/10.1016/j.enganabound.2014.06.005.

Sasaki, T., I. Hagiwara, K. Sasaki, R. Yoshinaka, Y. Ohnishi, S. Nishiyama, and T. Koyama. 2011. "Stability analyses for ancient masonry structures using discontinuous deformation analysis and numerical manifold method." *Int. J. Comput. Meth.* 8 (2): 247–275. https://doi.org/10.1142/S0219876211002575.

Shi, G. H. 1988. "Discontinuous deformation analysis: A new numerical model for the statics and dynamics of block systems." Ph.D. thesis. Dept. of Civil Engineering, Univ. of California, Berkeley. https://doi.org/10.1108/eb023855.

Shi, G. H. 1991. "Manifold method of material analysis." In *Transactions of the 9th Army Conf. on Applied Mathematics and Computing*. Rep. No. 92-1, 57–76. Minneapolis: US Army Research Office.

Shi, G. H. 2015. "Contact theory." *Sci. China Technol. Sci.* 58 (9): 1450–1498. https://doi.org/10.1007/s11431-015-5814-3.

Tsesarsky, Y., and Y. H. Hatzor. 2006. "Tunnel roof deflection in blocky rock masses as a function of joint spacing and friction—A parametric study using discontinuous deformation analysis (DDA)." *Tunnelling Underground Space Technol.* 21 (1): 29–45. https://doi.org/10.1016/j.tust.2005.05.001.

Wei, W., Q. H. Jiang, and J. Peng. 2016. "New rock bolt model and numerical implementation in numerical manifold method." *Int. J. Geomech.* 17 (5): E4016004. https://doi.org/10.1061/(ASCE)GM.1943-5622.0000669.

Wong, L. N. Y., and Z. Wu. 2014. "Application of the numerical manifold method to model progressive failure in rock slopes." *Eng. Fract. Mech.* 119: 1–20. https://doi.org/10.1016/j.engfracmech.2014.02.022.

Wu, J. H. 2007. "Applying discontinuous deformation analysis to assess the constrained area of the unstable Chiu-fen-erh-shan landslide slope." *Int. J. Numer. Anal. Methods Geomech.* 31 (5): 649–666. https://doi.org/10.1002/nag.548.

Yan, C., and H. Zheng. 2017a. "FDEM-flow3D: A 3D hydro-mechanical coupled model considering the pore seepage of rock matrix for simulating three-dimensional hydraulic fracturing." *Comput. Geotech.* 81: 212–228. https://doi.org/10.1016/j.compgeo.2016.08.014.

Yan, C., and H. Zheng. 2017b. "Three-dimensional hydromechanical model of hydraulic fracturing with arbitrarily discrete fracture networks using finite-discrete element method." *Int. J. Geomech.* 17 (6): 04016133. https://doi.org/10.1061/(ASCE)GM.1943-5622.0000819.

Yang, Y. T., G. H. Sun, H. Zheng, and X. D. Fu. 2016a. "A four-node quadrilateral element fitted to numerical manifold method with continuous nodal stress for crack analysis." *Comput. Struct.* 177: 69–82. https://doi.org/10.1016/j.compstruc.2016.08.008.

Yang, Y. T., X. H. Tang, H. Zheng, Q. S. Liu, and L. He. 2016b. "Three-dimensional fracture propagation with numerical manifold method." *Eng. Anal. Bound. Elem.* 72: 65–77. https://doi.org/10.1016/j.enganabound.2016.08.008.

Yang, Y. T., X. H. Tang, H. Zheng, Q. S. Liu, and Z. J. Liu. 2018. "Hydraulic fracturing modeling using the enriched numerical manifold method." *Appl. Math. Model.* 53: 462–486. https://doi.org/10.1016/j.apm.2017.09.024.

Yang, Y. T., D. D. Xu, G. H. Sun, and H. Zheng. 2017a. "Modeling complex crack problems using the three-node triangular element fitted to numerical manifold method with continuous nodal stress." *Sci. China. Technol. Sci.* 60 (10): 1537–1547. https://doi.org/10.1007/s11431-016-0733-4.

Yang, Y. T., and H. Zheng. 2016. "A three-node triangular element fitted to numerical manifold method with continuous nodal stress for crack analysis." *Eng. Fract. Mech.* 162: 51–75. https://doi.org/10.1016/j.engfracmech.2016.05.007.

Yang, Y. T., and H. Zheng. 2017. "Direct approach to treatment of contact in numerical manifold method." *Int. J. Geomech.* 17 (5): E4016012. https://doi.org/10.1061/(ASCE)GM.1943-5622.0000714.

Yang, Y. T., H. Zheng, and M. V. Sivaselvan. 2017b. "A rigorous and unified mass lumping scheme for higher-order elements." *Comput. Methods Appl. Mech. Eng.* 319: 491–514. https://doi.org/10.1016/j.cma.2017.03.011.

Yeung, M. R., Q. H. Jiang, and N. Sun. 2003. "Validation of block theory and three-dimensional discontinuous deformation analysis as wedge stability analysis methods." *Int. J. Rock. Mech. Min. Sci.* 40 (2): 265–275. https://doi.org/10.1016/S1365-1609(02)00137-5.

Yeung, M. R., Q. H. Jiang, and N. Sun. 2007. "A model of edge-to-edge contact for three-dimensional discontinuous deformation analysis." *Comput. Geotech.* 34 (3): 175–186. https://doi.org/10.1016/j.compgeo.2006.11.001.

Yu, Y., and J. Yin. 2015. "Some modifications to the process of discontinuous deformation analysis." *J. Rock Mech. Geotech. Eng.* 7 (1): 95–100. https://doi.org/10.1016/j.jrmge.2014.12.001.

Zhang, G. X., Y. Zhao, and X. C. Peng. 2010. "Simulation of toppling failure of rock slope by numerical manifold method." *Int. J. Comput. Meth.* 7 (1): 167–189. https://doi.org/10.1142/S0219876210002118.

Zhang, Y. H., X. D. Fu, and Q. Sheng. 2014. "Modification of the discontinuous deformation analysis method and its application to seismic response analysis of large underground caverns." *Tunnelling Underground Space Technol.* 40: 241–250. https://doi.org/10.1016/j.tust.2013.10.012.

Zheng, F., Y. Y. Jiao, X. L. Zhang, F. Tan, L. Wang, and Q. Zhao. 2017. "Object oriented contact detection approach for three-dimensional discontinuous deformation analysis based on entrance block theory." *Int. J. Geomech.* 17 (5): E4016009. https://doi.org/10.1061/(ASCE)GM.1943-5622.0000718.

Zheng, H., and W. Jiang. 2009. "Discontinuous deformation analysis based on complementary theory." *Sci. China Ser. E: Technol. Sci.* 52 (9): 2547–2554. https://doi.org/10.1007/s11431-009-0256-4.

Zheng, H., and X. K. Li. 2015. "Mixed linear complementarity formulation of discontinuous deformation analysis." *Int. J. Rock Mech. Min.* 75: 23–32. https://doi.org/10.1016/j.ijrmms.2015.01.010.

Zheng, H., F. Liu, and X. L. Du. 2015a. "Complementarity problem arising from static growth of multiple cracks and MLS-based numerical manifold method." *Comput. Methods Appl. Mech. Eng.* 295: 150–171. https://doi.org/10.1016/j.cma.2015.07.001.

Zheng, H., Z. J. Liu, and X. R. Ge. 2013. "Numerical manifold space of Hermitian form and application to Kirchhoff's thin plate problems." *Int. J. Numer. Methods Eng.* 95 (9): 721–739. https://doi.org/10.1002/nme.4515.

Zheng, H., F. Liu, and C. Li. 2014a. "The MLS-based numerical manifold method with applications to crack analysis." *Int. J. Fracture.* 190 (1–2): 147–166. https://doi.org/10.1007/s10704-014-9980-2.

Zheng, H., F. Liu, and C. Li. 2015b. "Primal mixed solution to unconfined seepage flow in porous media with numerical manifold method." *Appl. Math. Model.* 39 (2): 794–808. https://doi.org/10.1016/j.apm.2014.07.007.

Zheng, H., and D. D. Xu. 2014. "New strategies for some issues of numerical manifold method in simulation of crack propagation." *Int. J. Numer. Methods Eng.* 97 (13): 986–1010. https://doi.org/10.1002/nme.4620.

Zheng, H., and Y. T. Yang. 2017. "On generation of lumped mass matrices in partition of unity based methods." *Int. J. Numer. Methods Eng.* 112 (8): 1040–1069. https://doi.org/10.1002/nme.5544.

Zhu, B. F. 2009. *The finite element method, theory, and applications* [In Chinese.] Beijing: China Water Resources and Hydropower Press.

Zhu, H., W. Wu, J. Chen, G. Ma, X. Liu, and X. Zhuang. 2016. "Integration of three dimensional discontinuous deformation analysis (DDA) with binocular photogrammetry for stability analysis of tunnels in blocky rock mass." *Tunnelling Underground Space Technol.* 51: 30–40. https://doi.org/10.1016/j.tust.2015.10.012.

Zienkiewicz, O. C., and R. L. Taylor. 2000. *The finite element method.* 5th ed. Oxford, UK: Butterworth-Heinemann.